FOREWORD

Since January 1961 the Crew Stations Section, Human Engineering Branch, Behavioral Sciences Laboratory, has been conducting research to determine man's ability to perform orbital rendezvous tasks using only visual cues. This research was prompted, in part, by the development of a prototype self-maneuvering unit for orbital maintenance workers designed for the Air Force by Vought Astronautics Division, Chance Vought Corporation, Ling-Temco-Vought, Inc. This report is the result of analytical studies performed between December 1961 and March 1962 in support of this research. The work was done under Project No. 7184, "Human Performance in Advanced Systems," Task No. 718405, "Design Criteria for Crew Stations in Advanced Systems.

ABSTRACT

The purpose of this report is to analyze the relative motion which exists between an interceptor and target vehicle in the final stages of orbital rendezvous. Four distinct types of nearby parking orbits were defined. It was assumed that a man wearing an extra-vehicular suit and a self-maneuvering unit would exit the interceptor and traverse the remaining distance to the target. Both two-impulse transfers and continuous-thrust, line-of-sight transfers were analyzed. It was found that the direction in which the man should aim himself to make a two-impulse transfer depends only on the time he wishes to consume in the rendezvous and does not depend on the distance to be traveled. Comparisons of fuel consumption for the two-impulse technique and the line-of-sight technique were made and an optimum transfer combining both these techniques was suggested. The results of this study indicate that Coriolis forces and tidal effects cannot be neglected even at the relatively short ranges associated with orbital docking.

PUBLICATION REVIEW

This technical documentary report has been reviewed and is approved.

Walter F. Grether

WALTER F. GRETHER
Technical Director
Behavioral Sciences Laboratory

RELATIVE MOTION IN THE DOCKING PHASE OF ORBITAL RENDEZVOUS

INTRODUCTION

In this report we outline a method for analyzing the relative motion between a target satellite and a rendezvous vehicle, and define nearby parking orbits from which an orbital worker could exit the rendezvous vehicle, translate to the target, and return to the rendezvous vehicle.

Future space missions will require man to perform inspection, maintenance, resupply, assembly, or rescue tasks on vehicles already in orbit. At the present time opinions vary on whether a rendezvous vehicle (hereafter referred to as the interceptor) should be "flown" into direct physical contact with the target satellite (hereafter referred to as the target). There are many reasons which could preclude mechanical coupling of the target and interceptor. Aside from the obvious dangers of an inadvertent collision in space, there is the possibility that the target would be noncooperative or would not possess compatible coupling hardware.

This report is concerned only with the case in which the interceptor will park near the target while a pressure-suited man exits the interceptor with a self-propulsion device and traverses the remaining distance to the target.

SECTION I

RELATIVE MOTION BETWEEN AN INTERCEPTOR AND A TARGET IN A CIRCULAR ORBIT

Coordinate Reference Frame

Before discussing the relative motion between the target and interceptor, it is necessary to establish a coordinate frame of reference to describe this motion. Hord (ref. 4) and Brissenden et al. (ref. 1) chose a coordinate system with origin at the target's center of mass and axes always parallel to lines fixed in inertial space. This constitutes a noninertial, nonrotating frame of reference. The coordinate system used in this report also has its origin at the target's center of mass, which we may assume, for the moment, is in a circular orbit, but the y-axis is chosen to be in the orbital plane coincident with the local vertical (figure 1). The x-axis is taken to be perpendicular to the y-axis, tangential to the target's orbit. The z-axis is perpendicular to the orbital plane to form a right-handed, rectangular coordinate system.

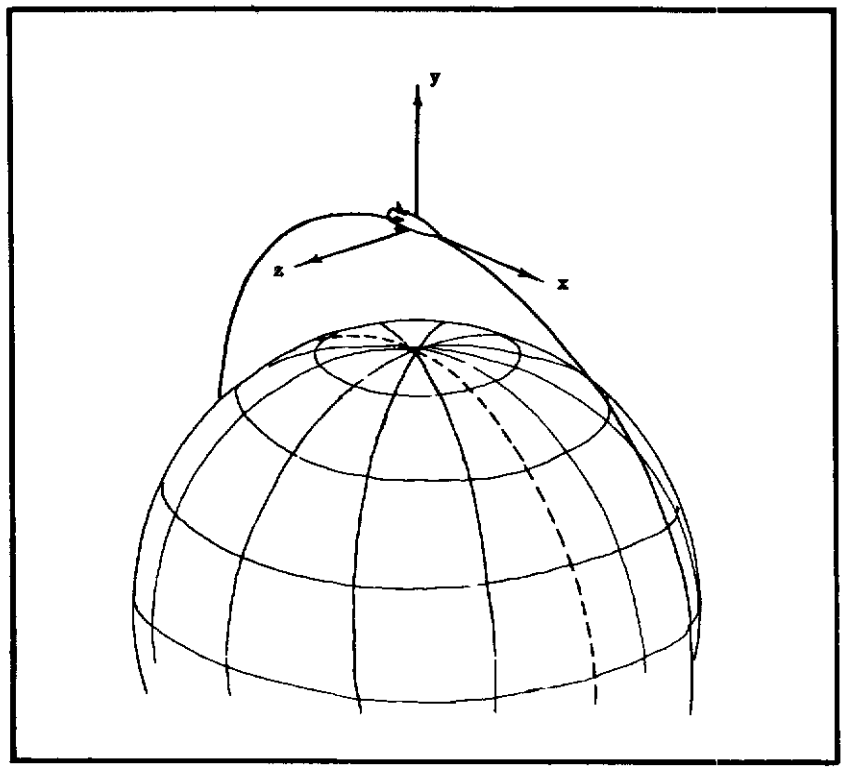

Figure 1. Coordinate System

The choice of a coordinate system fixed with respect to the local vertical seems logical since man is accustomed to thinking of the earth as establishing his "fixed directions." The earth will still be the most predominant feature of the space landscape for low earth orbits. From a 200-nautical-mile circular orbit the horizon will be depressed 19 degrees from the horizontal and will appear highly curved (figure 2). For the portion of the orbit which lies over the darkened side of the earth, the horizon will still be apparent as a black void in the stellar background. The stars will appear to rise or set once every 92 minutes and the earth will appear to be rotating under the orbiting observer.

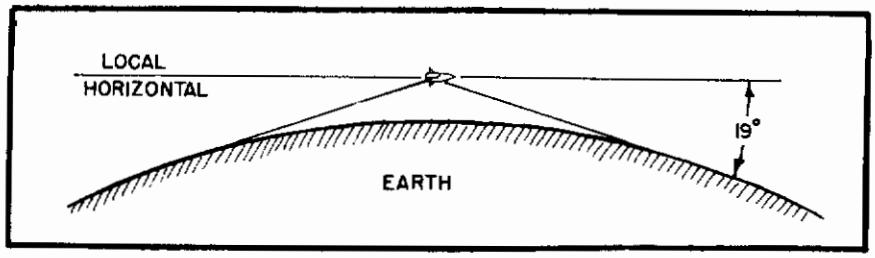

Figure 2. Depression of the Horizon from a 200-Nautical-Mile Orbit

Equations of Motion

If we assume that the distance between the target and interceptor is always small compared to the distance from the target to the center of the earth, we obtain the following linearized equations of motion (see Appendix, Derivation of Equations of Motion):

$$\ddot{x} = f_x - 2\omega\dot{y} \tag{1}$$

$$\ddot{y} = f_y + 2\omega\dot{x} + 3\omega^2 y \tag{2}$$

$$\ddot{z} = f_z - \omega^2 z \tag{3}$$

where:

$\ddot{x}$, $\ddot{y}$, and $\ddot{z}$ = x-, y-, and z-accelerations of the interceptor

f_x, f_y, and f_z = x-, y-, and z-components of external force per unit mass on the interceptor (exclusive of gravity)

$\dot{x}$ and $\dot{y}$ = x- and y-velocities of the interceptor

ω = angular velocity of the rotating coordinate system relative to inertial space. (For a 200-nautical-mile orbit, ω = 0.00114 radian/second.)

Terms other than external forces appear on the right-hand side of these equations. This is due to the fact that we have chosen a noninertial, rotating reference frame for our coordinate system. Newton's laws of motion do not apply in such a system, but, if we imagine that the accelerations described by these terms are due to "pseudo-forces," then we can apply Newton's laws as before. These are not true forces in that they do not represent attractions or repulsions of one body on another, but, rather, are a consequence of working in a noninertial coordinate system.

The second (ω) terms on the right-hand side of equations 1 and 2 are associated with the Coriolis effect and will be referred to as Coriolis terms.

The third (ω^2) term on the right-hand side of equation 2 represents the difference between gravitational and centrifugal accelerations acting on the interceptor. This term will be referred to as the "tidal" term for reasons to be explained later.

In the linearized equations (1, 2, and 3), x and y (in-plane) motions are not coupled to z (out-of-plane) motions, and so it is possible to discuss the in-plane and out-of-plane motions separately.

Relative Motion in the Orbital Plane

Qualitative Discussion of Equations of Motion:

Equations 1 and 2 describe the relative motion of the interceptor and the target in the orbital plane of the target. If we assume that f_x and f_y are both zero (no net thrust acting on the interceptor), we are left with:

$$\ddot{x} = -2\omega\dot{y} \tag{4}$$

$$\ddot{y} = 2\omega\dot{x} + 3\omega^2 y \tag{5}$$

We see immediately that a true parking orbit (one where the relative velocity between target and interceptor is zero) can exist only if both $\dot{x}$ and $\dot{y}$ are zero and there is no displacement of the interceptor in the y (vertical) direction. If these conditions are met, then both $\ddot{x}$ and $\ddot{y}$ are zero and the interceptor remains stationary relative to the target. This amounts to having the interceptor in the same-size circular orbit as the target and displaced any distance ahead of or behind the target.

We also see, however, that this is a condition of unstable equilibrium. Any slight displacement of the interceptor from the target's altitude in the vertical direction will subject the interceptor to a tidal force which will force it farther from the target's altitude.

If the interceptor has components of velocity in either or both the x- and y-directions, Coriolis forces act at right angles to the relative velocity vector (in the plane of the orbit) causing the interceptor's path to be curved. If the direction of orbital motion (positive x-axis) is drawn to the right, the interceptor's path will always curve in the counterclockwise direction as shown in figure 3. Since the Coriolis force always acts at right angles to the relative velocity vector, it cannot change the speed of the interceptor but can change its direction. This fact will become important in later energy analyses.

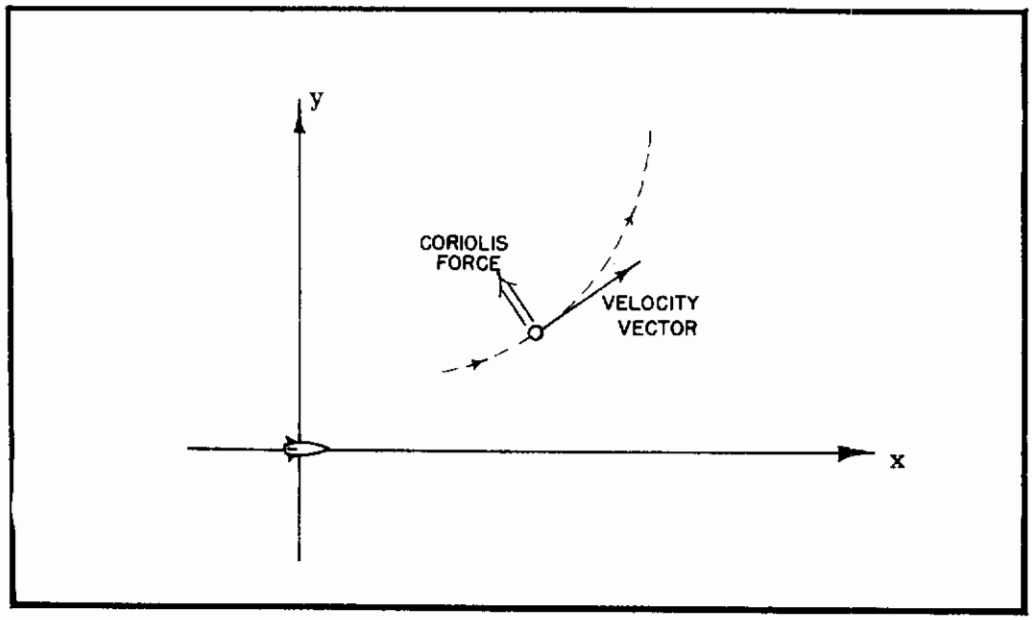

Figure 3. Effect of Coriolis Forces on the Interceptor's Trajectory

We have already noted that, if the interceptor is displaced vertically in the plus or minus y-direction, the tidal term in equation 5 causes the interceptor to be forced farther away from the target's altitude. The effect of the tidal term is the same as if there were a force field repelling the interceptor from the y = 0 line (figure 4). An identical term in the equations of motion of the earth around the sun accounts for the solar tides in the earth's ocean. Lunar tides, which are much stronger, have a similar explanation (ref. 2). Figure 5 illustrates how an imbalance between centrifugal and gravity forces can raise tidal bulges in the earth's oceans. If the earth is assumed to be in a circular orbit about the sun, then only the center of mass of the earth has exactly circular velocity. An ocean particle at A (figure 5) has slightly more than circular velocity and tends to rise to a greater distance from the sun because centrifugal forces overbalance the gravity forces. Similarly, an ocean particle at B (figure 5) has slightly less than circular velocity and tends to fall in nearer to the sun. The result is the familiar tidal bulges both toward and away from the sun.

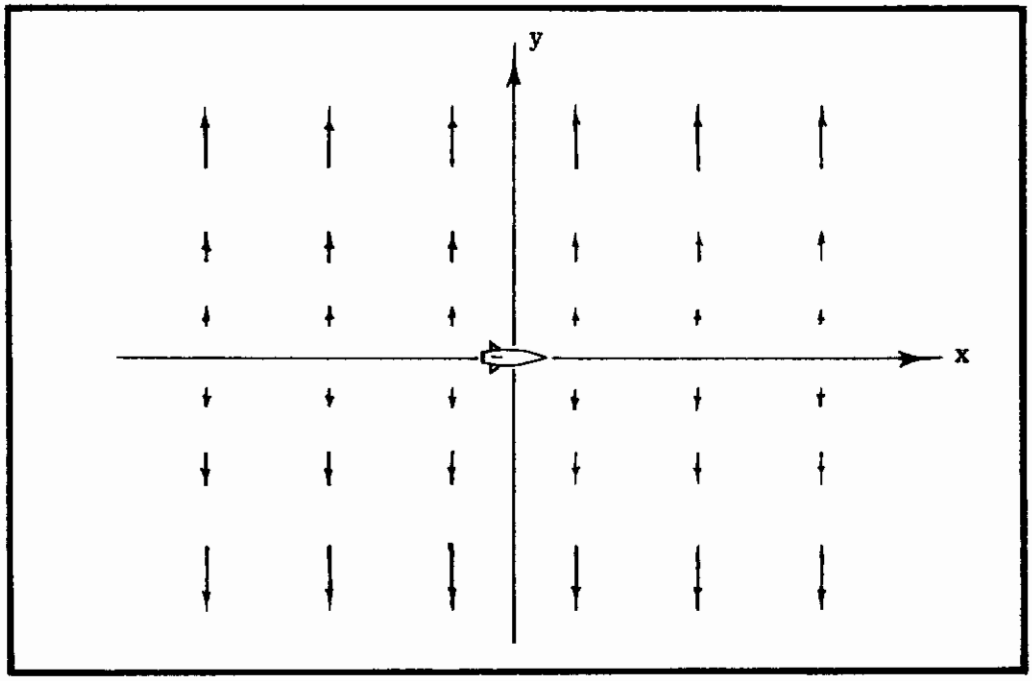

Figure 4. Tidal Force Field

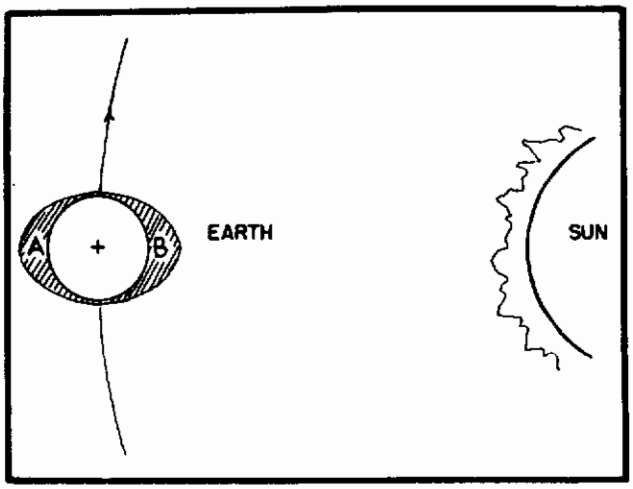

Figure 5. Tide-Generating Effect of the Sun

Analytical Solution of Equations of Motion:

We have seen qualitatively how the interceptor's motion will be affected by both Coriolis and tidal forces. To determine exactly how the interceptor will move under the influence of both of these perturbations, it is necessary to analytically solve equations 4 and 5.

If we do this we find:

$$x = (x_o - \frac{2\dot{y}_o}{\omega}) + (-3\dot{x}_o - 6\omega y_o)t - 2(-3y_o - 2\frac{\dot{x}_o}{\omega})\sin\omega t + 2(\frac{\dot{y}_o}{\omega})\cos\omega t \quad (6)$$

$$y = (4y_o + 2\frac{\dot{x}_o}{\omega}) + (-3y_o - 2\frac{\dot{x}_o}{\omega})\cos\omega t + (\frac{\dot{y}_o}{\omega})\sin\omega t \quad (7)$$

where:

x_o and y_o = initial values of x and y at time zero

$\dot{x}_o$ and $\dot{y}_o$ = initial values of x- and y-velocity at time zero

t = time

Geometrical Interpretation of Analytical Solution:

While these equations appear complicated, a simple geometrical interpretation makes them quite tractable. It can be shown that equations 6 and 7 describe a point moving on an ellipse the major axis of which is twice its minor axis regardless of initial conditions. The center of the ellipse is at:

$$x_c = x_o - \frac{2\dot{y}_o}{\omega} \quad (8)$$

$$y_c = 4y_o + \frac{2\dot{x}_o}{\omega} \quad (9)$$

and the center is drifting in the x-direction with a velocity of:

$$v_c = -3(\dot{x}_o + 2\omega y_o) \quad (10)$$

The size of the drifting ellipse is dependent on $\dot{y}_o$, $\dot{x}_o$, and y_o, but is independent of x_o. The semi-minor axis, b, of the ellipse is given by:

$$b = \sqrt{(\frac{\dot{y}_o}{\omega})^2 + (3y_o + 2\frac{\dot{x}_o}{\omega})^2} \quad (11)$$

The semi-major axis, a, is just:

$$a = 2b \quad (12)$$

Figure 6 illustrates the geometry of the situation. The drifting ellipse is shown with its center initially at (x_c, y_c) and drifting in the x-direction with velocity, v_c. At the same time the interceptor at point I is moving in a counterclockwise direction around the perimeter of the moving ellipse, making one complete circuit around the perimeter in one orbital period.

The y-displacement of the center of the drifting ellipse is significant because it tells us whether the interceptor is in an orbit of the same period as that of the target. Note from equations 9 and 10 that, if y_c is zero, the drift velocity, v_c, of the ellipse is also zero and the interceptor returns to the point from which it started after one orbital period. If the center of the ellipse is above the target's altitude, the ellipse has a drift velocity in the negative x-direction. Conversely, if the center is below the target altitude, the ellipse drifts in the positive x-direction.

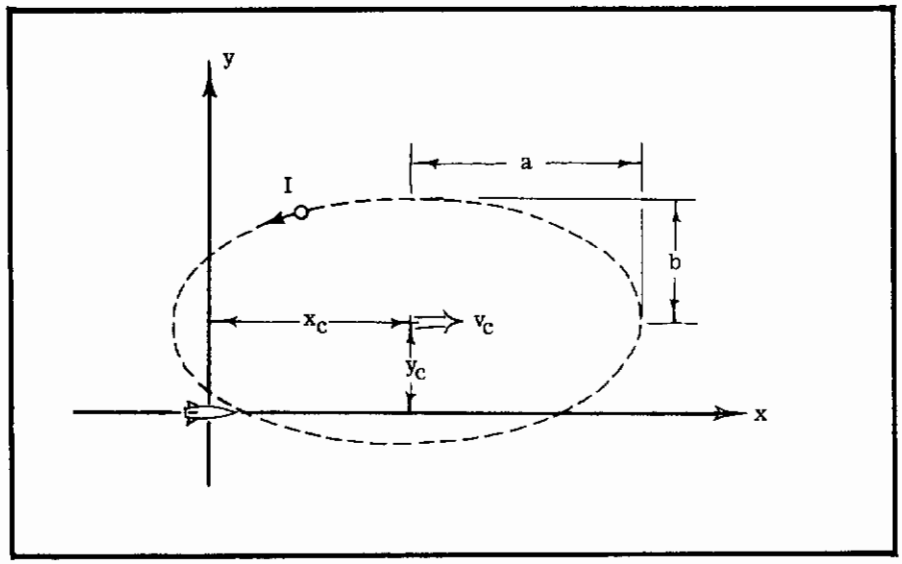

Figure 6. Drifting Ellipse Which Generates the Trajectory of the Interceptor

From an initial position (x_o, y_o), for the interceptor to enter an orbit the period of which is the same as that of the target, the following conditions must be met:

$$y_C = 4y_o + \frac{2\dot{x}_o}{\omega} = 0 \tag{13}$$

or:

$$\dot{x}_o = -2\omega y_o \tag{14}$$

If we take as an example a target in a 200-nautical-mile circular orbit, so that $\omega = 0.00114$ radian per second, and assume that the interceptor starts from a position 2000 feet ahead of and 2000 feet above the target, the proper x-velocity is -4.56 feet per second. Trajectory number 1 in figure 7 shows the path of the interceptor starting from this position with a velocity of 4.56 feet per second in the minus x-direction and zero velocity in the y-direction. Note that the path of the interceptor is an ellipse centered at the target's altitude and 2000 feet ahead of the target. The initial y-velocity does not affect the orbital period of the interceptor. Trajectories 2 and 3 in figure 7 show the effect of arbitrary velocities of plus and minus 2 feet per second in the y-direction. In each case the elliptical path produced has its center on the target's altitude. It is possible, however, by adjusting the initial y-velocity, to obtain an ellipse centered at the target itself. The correct y-velocity may be obtained from equation 8 by setting x_C equal to zero. The required value of $\dot{y}_o$ is:

$$\dot{y}_o = \frac{\omega x_o}{2} \tag{15}$$

For the example we have chosen, $\dot{y}_o$ must be 1.14 feet per second for a target-centered parking orbit. Figure 8 shows the path which results.

A special case occurs when both a and b are zero, or, in other words, the drifting ellipse has shrunk to zero size.

Equation 11 tells us that this can occur only if $\dot{y}_c = 0$

and $$\dot{x}_o = -\tfrac{3}{2}\omega y_o \tag{16}$$

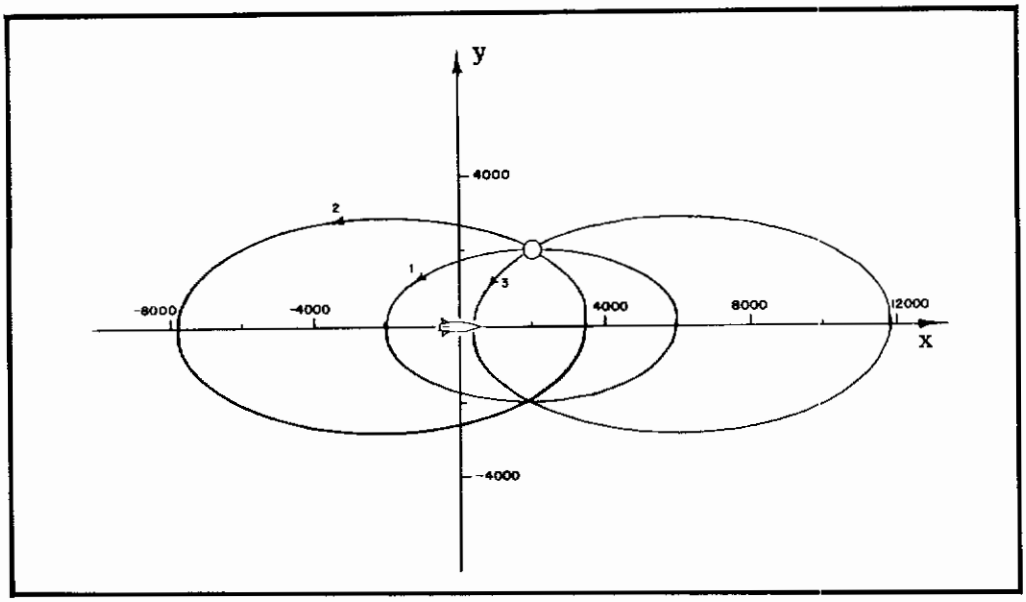

Figure 7. Ellipse Centered at Target's Altitude

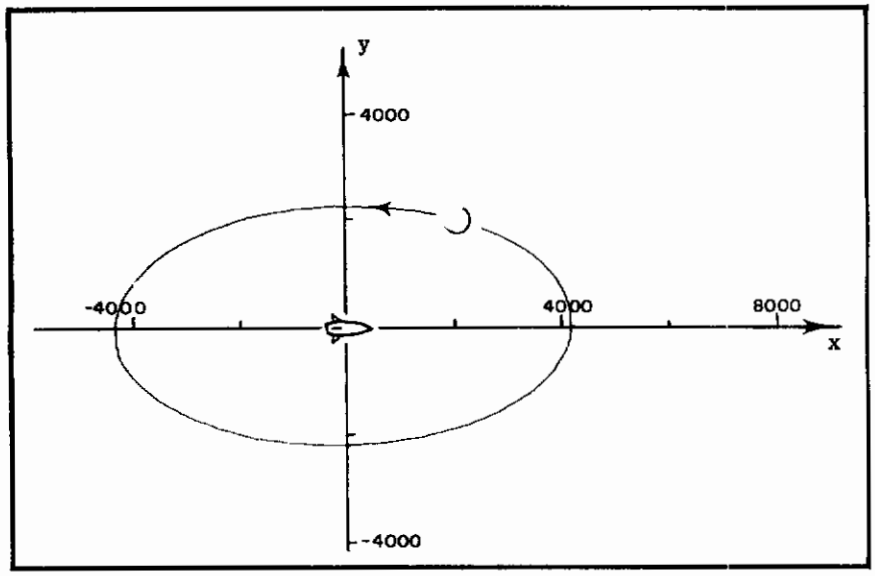

Figure 8. Target-Centered Parking Orbit

It is not difficult to show that this situation corresponds to having the interceptor in a circular orbit. If the interceptor is initially 8000 feet ahead of the target and 2000 feet above it, we can compute from equation 16 that a velocity of -3.42 feet per second in the x-direction and $\dot{y}_0$ equal to zero will put the interceptor into a circular orbit 2000 feet higher than the target. Trajectory 1 in figure 9 illustrates the path of the interceptor during one orbital period of the target. Note that the interceptor drifts horizontally and falls 18,900 feet behind the target after 92 minutes. If the interceptor had started 2000 feet below the target and had an initial velocity of 3.42 feet per second in the positive x-direction, it would have drifted horizontally in the forward direction at the same rate.

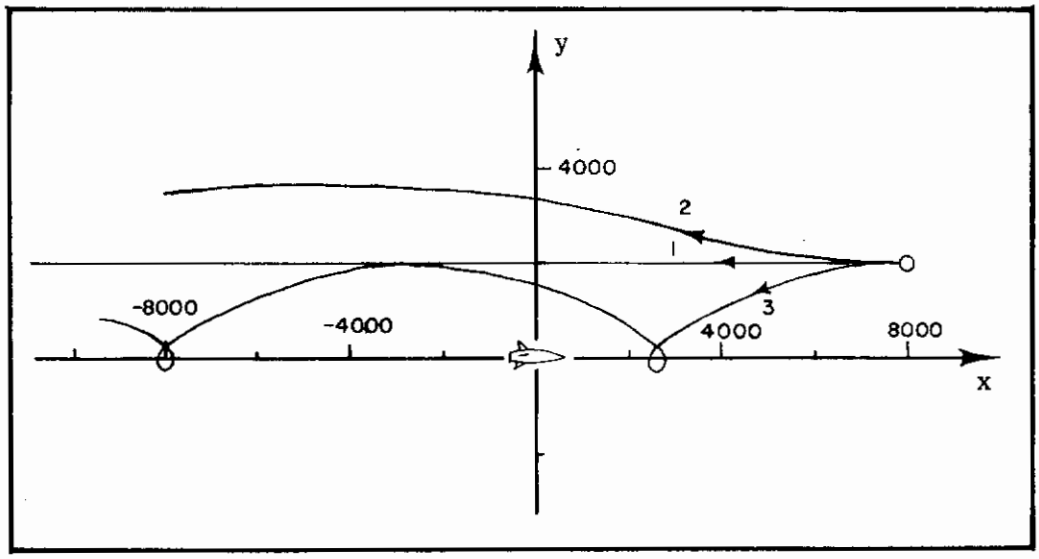

Figure 9. Interceptor in Circular and Nearly Circular Orbits

The consequences of having slightly more or less than the proper circular velocity are illustrated in trajectories 2 and 3, figure 9. If the interceptor has 0.5 foot per second in excess of circular velocity (x_o = -2.92 feet per second), the path (trajectory 2) undulates as the interceptor rises toward its apogee and then falls back toward perigee, all the while falling farther and farther behind the target. Trajectory 3 shows what happens if the interceptor has 0.5 foot per second less than circular velocity ($\dot{x}_o$ = -3.92 feet per second). As it falls toward perigee, it gains enough speed to momentarily be overtaking the target. However, as it rises toward apogee again, it falls behind; hence, it follows a distorted cycloidal path.

A special case of this cycloidal motion occurs if the interceptor starts initially at rest with respect to the target but slightly above or below the target's altitude. This situation might occur if the interceptor were attempting to enter a circular orbit at the target's altitude but inadvertently missed the target's altitude by a few hundred feet. Figure 10 (trajectory 1) shows the interceptor starting from rest at a position 8000 feet ahead of and 250 feet above the target. The cusp-shaped path is a consequence of the interceptor's having exactly zero velocity in the xy-coordinate system at its perigee point. If the interceptor starts 8000 feet behind and 500 feet below the target, trajectory 2 results. In this case, the interceptor has exactly zero velocity in the xy-coordinate system at the apogee of its orbit.

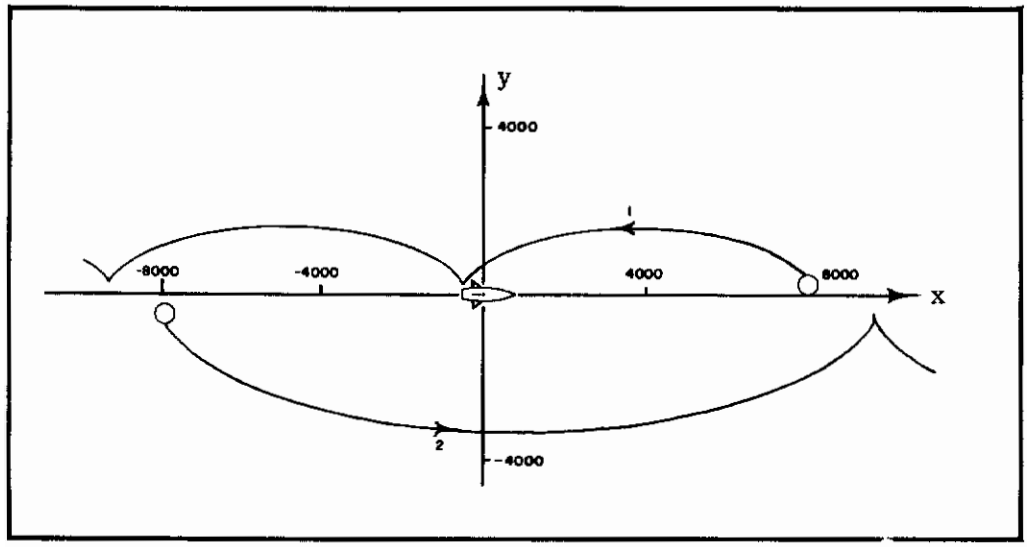

Figure 10 Interceptor Starting from Rest

To summarize the results of this geometrical interpretation, we can say that the coasting trajectory of the interceptor is traced out by a point moving on the perimeter of an ellipse the center of which may be drifting. If the interceptor happens to be in a circular orbit, the size of the drifting ellipse shrinks to zero. If the orbital period of the interceptor is the same as that of the target, the center of the ellipse will be on the x-axis, and the drift velocity will be zero. If the orbital period is longer, the center will be above the target's altitude and drifting backward. If the period is shorter, the center will be below the target and drifting forward.

Classification of Orbits

In discussing the coasting trajectory of the interceptor, the possible orbits could conveniently be classified into four general types. Table I illustrates the classification scheme used in this report. The criteria which determine the orbit type are whether the target and interceptor have the same or different orbital eccentricity and period.

TABLE I

CLASSIFICATION OF PARKING ORBITS

Orbit Type	Eccentricity		Period		Typical Trajectory	Remarks
	Same As Target	Not Same As Target	Same As Target	Not Same As Target		
I	X		X		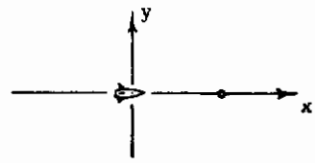	Interceptor remains stationary with respect to target in a condition of unstable equilibrium.
II		X	X		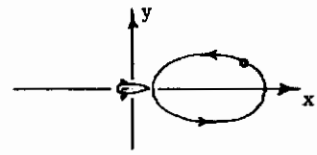	Interceptor always returns to its starting point after one orbital period.
III	X			X	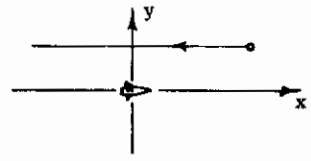	Interceptor drifts in a straight-line horizontal path relative to the target. Not a true parking orbit.
IV		X		X	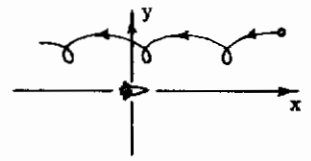	Interceptor traverses an ellipse whose center is drifting. Not a true parking orbit.

A type I orbit is one in which the interceptor has the same eccentricity and same period as the target. Since the target is in a circular orbit, the interceptor is in a circular orbit at the target's altitude. This represents the ideal parking situation if a man is to exit the interceptor and travel to the target and return, since the interceptor maintains the same relative position and zero relative velocity indefinitely without the expenditure of fuel.

In a type II orbit the interceptor has a slightly different eccentricity but the same period as the target. This corresponds to having the interceptor in an elliptical orbit. The fact that the period is the same insures that the interceptor will remain in the vicinity of the target and return to the same relative position and velocity at the end of each orbital period.

A type III orbit exists if the target and interceptor have the same eccentricity but different periods. This would be the case if the interceptor were in a circular orbit at some higher or lower altitude. This is not a true parking situation since the interceptor continues to drift behind or ahead of the target in a horizontal, straight-line path.

If both eccentricity and period are different for the interceptor and target, a type IV orbit results. The distorted cycloidal motion which ensues is clearly an undesirable parking situation.

Kinetic and Potential Energy of the Interceptor

While it is possible to obtain an expression for the speed of the interceptor by differentiating equations 6 and 7, we can obtain useful information by a simple energy analysis of the situation. Recall that the Coriolis forces always act at right angles to the interceptor's direction of motion. As a result, Coriolis forces can have no effect on the speed of the interceptor, but only act to change its direction. The tidal force field illustrated in figure 4 is a conservative field which means that we can assign a potential energy (P.E.) to the interceptor at any position and say that the sum of the interceptor's kinetic and potential energies must remain constant in the absence of external forces acting on the interceptor. The P.E. per unit mass of the interceptor is given by:

$$\text{P.E.} = -\tfrac{3}{2}\omega^2 y^2$$

while the kinetic energy (K.E.) per unit mass is:

$$\text{K.E.} = \tfrac{1}{2}(\dot{x}^2 + \dot{y}^2) = \tfrac{1}{2}v^2$$

where v is the speed of the interceptor in the xy-coordinate system.

Since the sum of K.E. and P.E. must remain constant, we can say that:

$$\tfrac{1}{2}v_1^2 - \tfrac{3}{2}\omega^2 y_1^2 = \tfrac{1}{2}v_2^2 - \tfrac{3}{2}\omega^2 y_2^2$$

where the subscript $_1$ refers to some initial time and the subscript $_2$ refers to some later time. The change in speed of the interceptor depends only on its change in altitude and can be obtained from the expression:

$$v_2^2 - v_1^2 = 3\omega^2(y_2^2 - y_1^2) \qquad (17)$$

To illustrate the use of this equation, consider an orbit of type II (see table I). If we take v_1 as the speed at which the interceptor crosses the target's altitude, and v_2 as its speed at apogee (figure 11), then it can be shown that v_2 is always twice v_1. If v_2 is chosen as the speed at perigee, the result is identical. In general, we can say that for orbits of type II the interceptor traces out an elliptical path in the xy-plane and crosses the target's altitude with half the speed that it possesses at apogee or perigee.

For orbits of type III, the altitude of the interceptor is constant, so we can conclude that the speed is constant.

In type IV orbits the interceptor is constantly exchanging speed for altitude. A particularly interesting example is illustrated in figure 10. At the end of one of the cusps in its trajectory, the interceptor has exchanged all of its kinetic energy for potential energy and is momentarily at rest in the xy-plane.

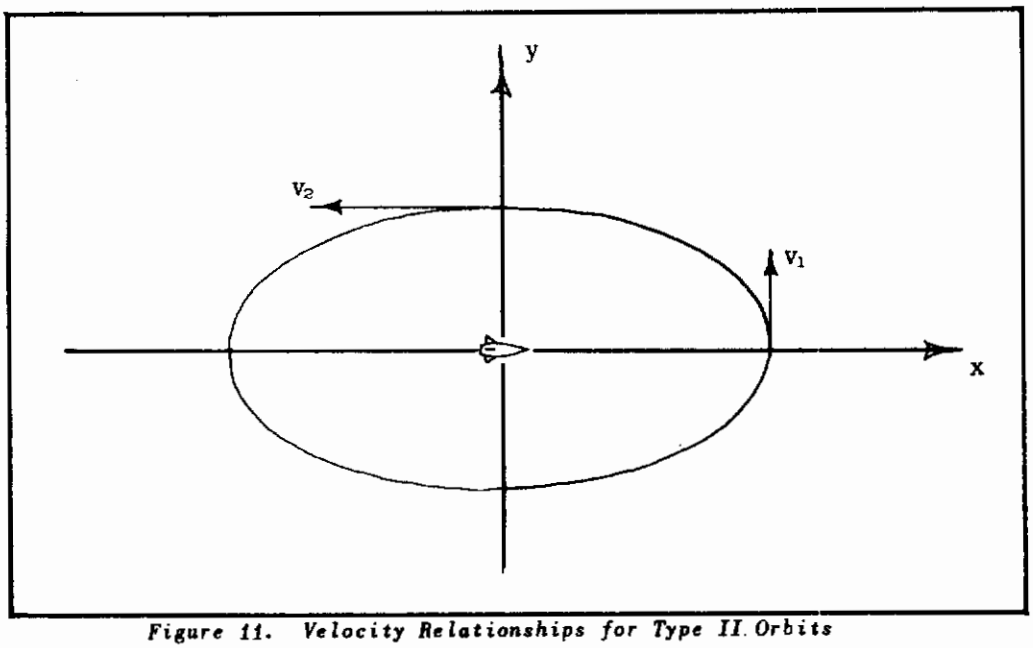

Figure 11. Velocity Relationships for Type II Orbits

Relative Motion out of the Orbital Plane

Equation 3 describes the noncoplanar motion of the interceptor. If we assume that f_z is zero (no net thrust acting in the z-direction), we are left with:

$$\ddot{z} = -\omega^2 z \tag{18}$$

The solution to equation 18 is simply:

$$z = \frac{\dot{z}_o}{\omega} \sin \omega t + z_o \cos \omega t \tag{19}$$

where:

z_o = initial value of z at time zero

$\dot{z}_o$ = initial value of z-velocity at time zero

A plot of z versus time is shown in figure 12. Note that the interceptor oscillates sinusoidally across the orbital plane, crossing through the plane of the target's orbit twice during each orbital period. Figure 13 illustrates why this must occur. If the interceptor is in a noncoplanar orbit, its orbit penetrates the orbital plane of the target (figure 13) at two points. For half of an orbital period the interceptor will be on one side of the target's orbital plane, and for the other half of the period, it will be on the opposite side.

The maximum excursion of the interceptor in the z-direction depends on the initial z-displacement and z-velocity of the interceptor, according to the relation:

$$z_{max} = \sqrt{\left(\frac{\dot{z}_o}{\omega}\right)^2 + z_o^2} \tag{20}$$

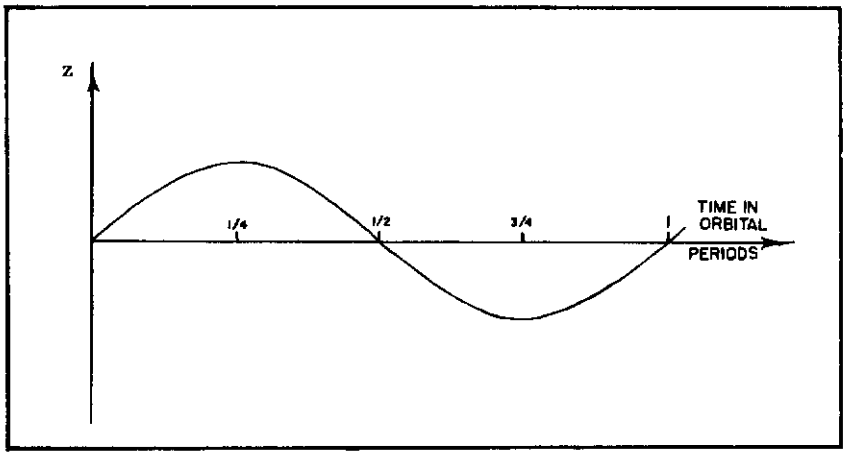

Figure 12. Displacement out of the Orbital Plane Versus Time

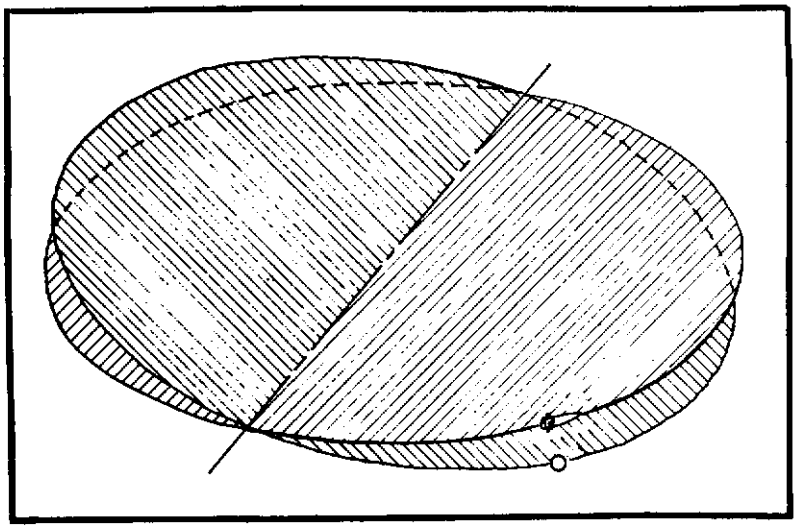

Figure 13. Noncoplanar Orbits

If the interceptor is in a noncoplanar orbit as shown in figure 13, the inclination, i, is related to z_{max} as follows (for small values of i):

$$i = \frac{z_{max}}{r_E + h} \qquad (21)$$

where:

i = inclination angle between the interceptor and target orbital planes, in radians

r_E = radius of the earth (3441.90 nautical miles)

h = altitude of target's orbit

If, for example, the target is in a 200-nautical-mile orbit and the interceptor's orbit is inclined $\frac{1}{2}$ degree (0.00873 radian) to the target's orbital plane, the interceptor will oscillate between maximum z-displacements of 31.79 nautical miles on either side of the target's orbital plane.

The interceptor will have its maximum velocity in the z-direction at the moment it passes through the target's orbital plane. This maximum velocity can be obtained from the initial conditions as follows:

$$\dot{z}_{max} = \omega z_{max} = \omega\sqrt{\left(\frac{\dot{z}_o}{\omega}\right)^2 + z_o^2} \qquad (22)$$

In the example just given, the maximum velocity would be 220 feet per second.

If the interceptor desires to enter a parking orbit in the vicinity of the target, the out-of-plane excursions must be kept to a minimum. This can be done by reducing the z-velocity to zero as the interceptor passes through the target's orbital plane. Each foot per second of z-velocity that the interceptor retains as it passes through the plane will result in an excursion of 877 feet to each side of the target.

Out-of-plane motions are completely independent of in-plane motions, provided, of course, that the distance between the target and interceptor never gets too large. Meyer (ref. 6) has shown that the linearized equations of motion are accurate to within 0.25 percent for distances as great as 20 miles. Hence, we can visualize the out-of-plane motion superimposed on the in-plane motion with no interaction between the two.

SECTION II

RELATIVE MOTION BETWEEN AN INTERCEPTOR AND A TARGET IN AN ELLIPTICAL ORBIT

Thus far we have restricted the target to a circular orbit at the center of the xyz-coordinate frame. Except in unusual cases, it is unlikely that the target's orbit will be exactly circular, so it is necessary to consider the more general case where the target is in an elliptical orbit.

Relative Motion in the Orbital Plane

Recall that originally we chose the origin of our coordinate frame to be at the target's center of mass. Equations 1, 2, and 3 then described the motion of the interceptor in this coordinate system. By saying that the target had to be in a circular orbit, we were really requiring that the origin of the coordinate frame move as though it were in a circular path. So long as the origin of the coordinate system moves in a circular path we can allow the target to be in an elliptical orbit and describe its motion in the xy-plane by means of equations 6 and 7, by using primed symbols to represent the parameters of the target.

$$x' = (x_o' - \frac{2\dot{y}_o'}{\omega}) + (-3\dot{x}_o' - 6\omega y_o')t - 2(-3y_o' - 2\frac{\dot{x}_o'}{\omega})\sin\omega t + 2(\frac{\dot{y}_o'}{\omega})\cos\omega t \quad (23)$$

$$y' = (4y_o' + 2\frac{\dot{x}_o'}{\omega}) + (-3y_o' - 2\frac{\dot{x}_o'}{\omega})\cos\omega t + (\frac{\dot{y}_o'}{\omega})\sin\omega t \quad (24)$$

As before, equations 6 and 7 describe the motion of the interceptor. In effect, what we have done is to describe the motion of the target and the interceptor, each relative to the xyz-frame which is in a circular orbit.

What we really want is to describe the motion of the interceptor relative to the target. This requires setting up a new $\xi\eta\zeta$-coordinate frame with the origin at the target and moving with it, but with the ξ-, η-, and ζ-axes always remaining parallel to the x-, y-, and z-axes, respectively.

To transform the equations of motion to the $\xi\eta\zeta$-frame, we need only apply the following simple relationships:

$$\xi = x - x'$$

$$\eta = y - y'$$

The resulting equations of motion, written in the target-centered frame, are:

$$\xi = (\xi_o - \frac{2\dot{\eta}_o}{\omega}) + (-3\dot{\xi}_o - 6\omega\eta_o)t - 2(-3\eta_o - 2\frac{\dot{\xi}_o}{\omega})\sin\omega t + 2(\frac{\dot{\eta}_o}{\omega})\cos\omega t \quad (25)$$

$$\eta = (4\eta_o + 2\frac{\dot{\xi}_o}{\omega}) + (-3\eta_o - 2\frac{\dot{\xi}_o}{\omega})\cos\omega t + (\frac{\dot{\eta}_o}{\omega})\sin\omega t \quad (26)$$

Note that these equations are mathematically identical in form to equations 6 and 7. Hence, the relative motion between the interceptor and the target is the same regardless of whether the target is in a circular or slightly elliptical orbit.

Recall that the linearized equations of motion are valid only if the distance between the interceptor and the origin of the xyz-frame is small compared to the distance between the origin of the

coordinate frame and the center of the earth. Similarly, the distance between the target and the origin of the xyz-frame must be kept small. If the xyz-frame is chosen so that the trajectory of the target in the xy-plane is an ellipse centered at the origin, then the maximum distance the target can get from the origin is simply the difference between the apogee and perigee altitudes of the target. If this distance is no greater than a few hundred nautical miles, equations 25 and 26 will be valid.

Since equations 25 and 26 are identical in form to equations 6 and 7, we need not further confuse the nomenclature by retaining the $\xi\eta\zeta$-coordinate frame.

Instead, let us consider the xyz-frame to be attached to the target as before and state that equations 6 and 7 are valid for the general case of the target in an elliptical orbit, provided that:

$$\omega = \frac{2\pi}{P} \tag{27}$$

where P is the orbital period of the target.

Furthermore, the classification scheme illustrated in table I is perfectly general and applies to the case where the target is in a slightly elliptical orbit.

SECTION III

TOTAL IMPULSE REQUIRED TO RENDEZVOUS FROM CLOSE-IN PARKING ORBITS

In the previous two sections we have established the general characteristics of close-in parking orbits. Let us now look at the problem of getting a pressure-suited man, wearing a self-maneuvering unit, from an interceptor in one of these parking orbits to the target.

Obviously, the amount of total impulse required depends on the thrust capabilities of the specific self-maneuvering unit and the rendezvous technique employed. Therefore, for the purposes of this report, let us assume that the man has a self-maneuvering unit such as was designed for the Air Force by Vought Astronautics Division (ref. 3). This unit, shown in figure 14, has ten fixed nozzles, giving the man both fore-aft and up-down thrust. It has automatic stabilization and can be commanded to give constant rate rotation in pitch, roll, and yaw by means of the hand-operated controller mounted on the stomach.

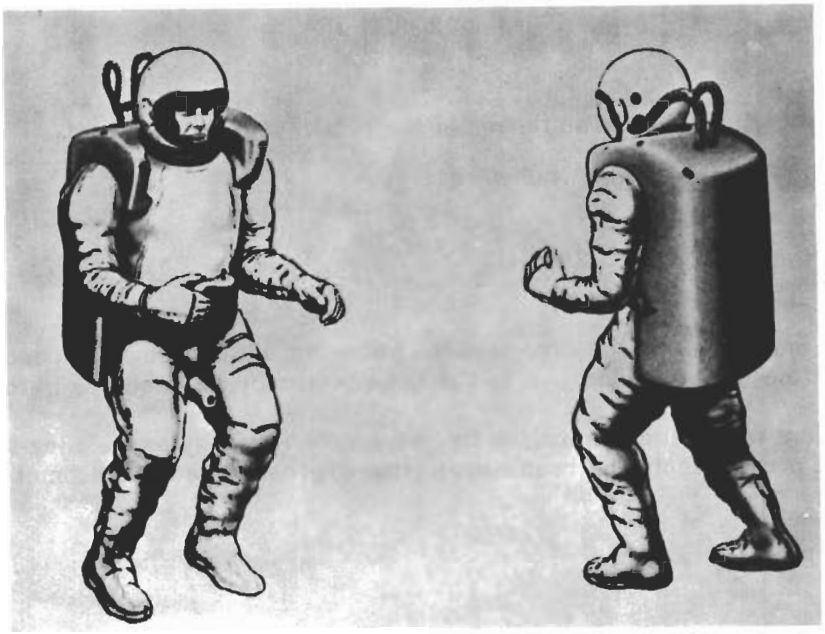

Figure 14. Typical Self-Maneuvering Unit

Rendezvous from Type I Parking Orbit

Type I parking orbits represent ideal starting conditions for missions where the astronaut must travel from the interceptor to the target and return at some later time. For this reason a rendezvous, starting from horizontally ahead of or behind the target and at rest relative to it, is the most likely and will be treated first.

The most efficient rendezvous technique from the standpoint of fuel consumption would be a two-impulse method. The astronaut would aim himself in the proper direction, apply a short burst of thrust to accelerate himself to some coasting velocity, and then coast in a trajectory which intercepts the target. Just prior to impact with the target, the astronaut would apply a short burst of retrothrust to bring himself to rest at the target.

It is customary to express the fuel consumed during such a maneuver in terms of total impulse per unit mass. This has the dimensions of a velocity and is often referred to as the Δv required.

The Δv required for a two-impulse rendezvous from a type I parking orbit is simply $2v$, where v is the coasting velocity.

To determine in which direction the astronaut should aim himself and what his coasting velocity should be, it is necessary to solve equations 6 and 7 for $\dot{x}_o$ and $\dot{y}_o$. The results are:

$$\dot{x}_o = -x_o \left[\frac{\omega}{8 \tan \left(\frac{\omega t_r}{2}\right) - 3\omega t_r} \right] \tag{28}$$

$$\dot{y}_o = 2x_o \left[\frac{\omega \tan \left(\frac{\omega t_r}{2}\right)}{8 \tan \left(\frac{\omega t_r}{2}\right) - 3\omega t_r} \right] \tag{29}$$

where t_r is the time elapsed from initiation of the rendezvous until impact.

The aiming angle, θ, is given by:

$$\tan \theta = \frac{\dot{y}_o}{\dot{x}_o} = -2 \tan \left(\frac{\omega t_r}{2}\right) \tag{30}$$

Equation 30 indicates that the direction the astronaut aims himself depends only on the time he wishes to consume in the rendezvous and is not affected by the distance which he has to travel.

It is convenient to nondimensionalize the rendezvous time by expressing it as a fraction of an orbital period. If p represents the rendezvous time expressed as a fraction of an orbital period, then:

$$p = \frac{\omega t_r}{2\pi} \tag{31}$$

Figure 15 shows how the aiming angle varies as a function of rendezvous time. Note that, for a rendezvous which takes half an orbital period, the astronaut aims himself 90° away from the target. For a rendezvous taking a full orbital period, he aims himself in the direction opposite the target regardless of his initial range.

The correct velocity to intercept the target depends on both the aiming angle and the initial range. This velocity may be obtained from equations 28, 30, and 31:

$$v = \frac{x_o \omega}{(4 \sin \theta + 6\pi p \cos \theta)} \tag{32}$$

and is plotted in figure 16.

While the two-impulse method represents the most economical rendezvous technique, Kasten (ref. 5) has found from rendezvous simulator studies that a line-of-sight technique is easier for a pilot to manage when only visual cues are available to aid him. This technique requires the astronaut to face directly at the target and apply forward thrust to obtain some closure velocity. The astronaut then uses orthogonal (up-down) thrust to overcome the Coriolis acceleration and keep himself on the straight line-of-sight path to the target. The amount of orthogonal thrust required to travel a horizontal straight line is plotted versus closure velocity in figure 17. Note that for

closure velocities of about 15 feet per second the orthogonal jets need supply only about three one-hundredths of a ft/sec^2 acceleration or only one-thousandth of a G. However, this must be applied continuously so long as the closure rate of 15 feet per second persists and can therefore result in significant Δv expenditures.

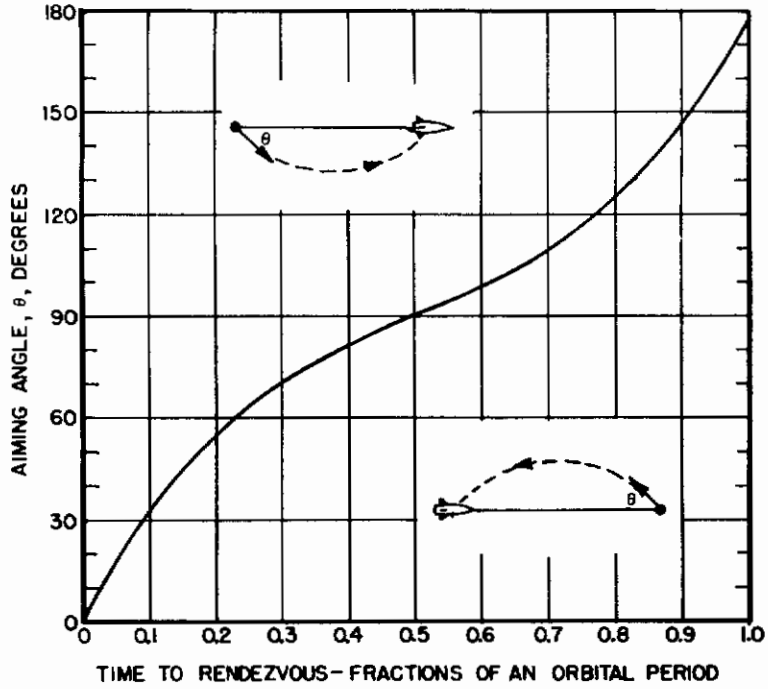

Figure 15. Relationship of Aiming Angle to Rendezvous Time for Type I Parking Orbits

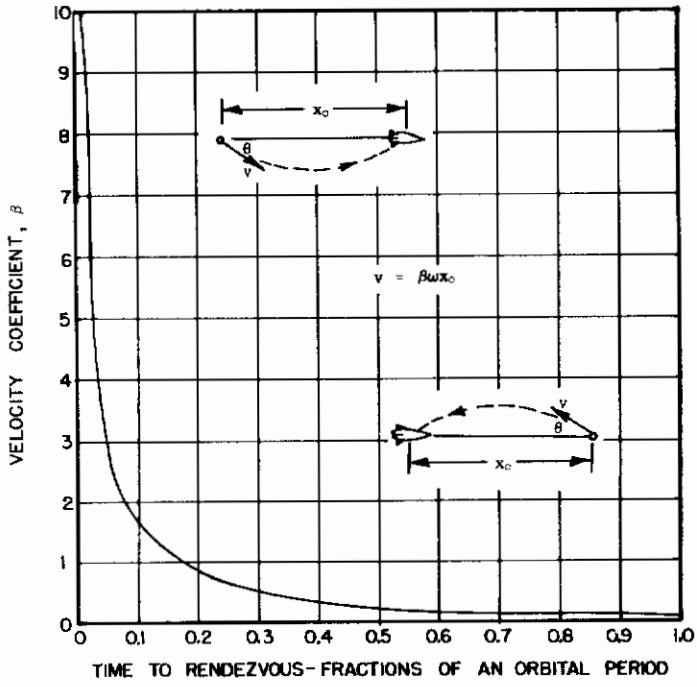

Figure 16. Relationship of Initial Coasting Velocity to Rendezvous Time for Type I Parking Orbits

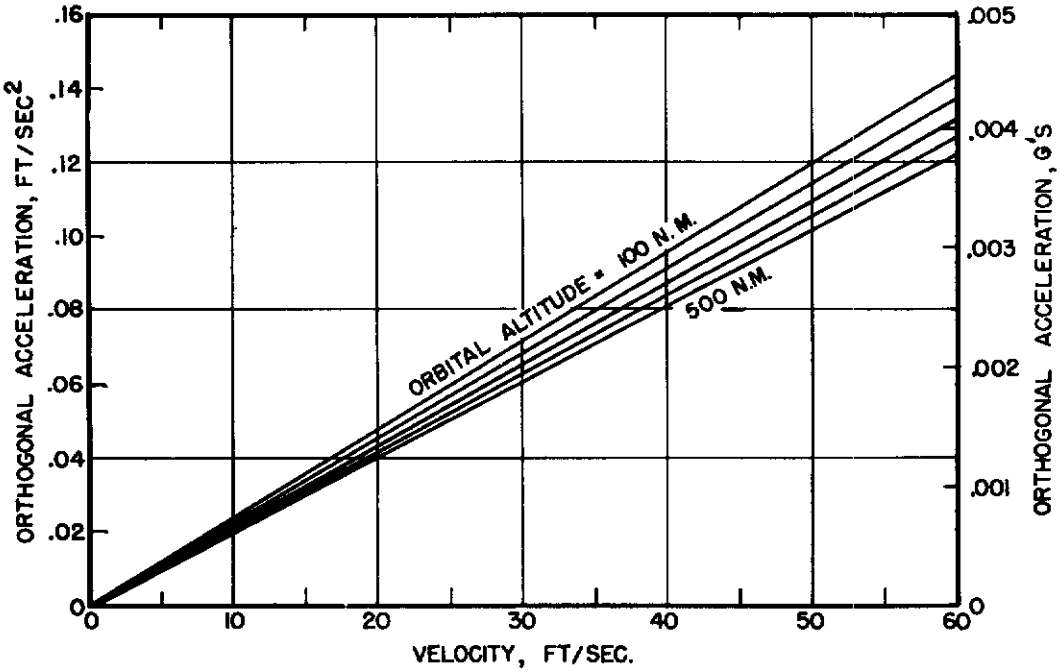

Figure 17. Orthogonal Thrust Required to Overcome Coriolis Acceleration

Since it is unlikely that orthogonal thrust levels as low as 0.001 G will be available, the astronaut can follow a zigzag path by applying 1-second bursts of orthogonal thrust at a level of 0.1 G every 100 seconds and accomplish essentially the same result.

The fuel consumed by the orthogonal jets depends only on the distance traveled in a straight line and is plotted in figure 18.

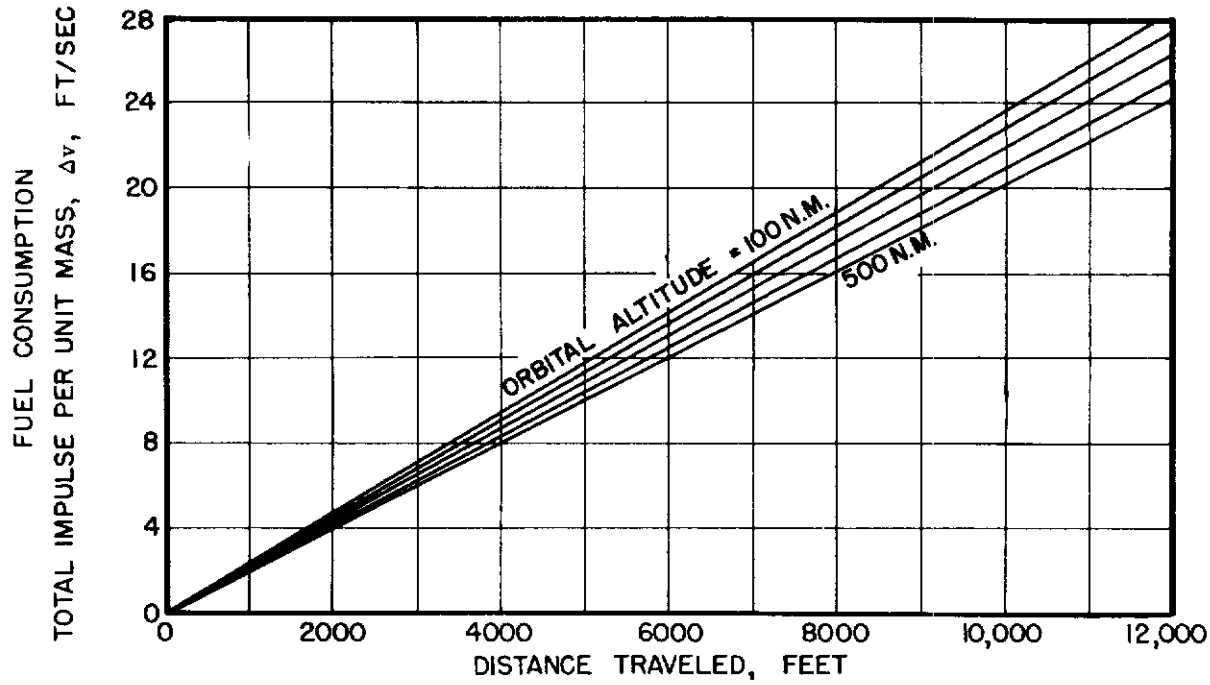

Figure 18. Fuel Required to Overcome Coriolis Acceleration

The total Δv consumed for a line-of-sight rendezvous is simply 2v (where v is the closure velocity) plus the Δv obtained from figure 18. The time-to-rendezvous is just:

$$t_r = \frac{x_o}{v} \tag{33}$$

where x_o is the initial range to the target.

The fuel penalty which must be paid to make the line-of-sight rendezvous rather than the two-impulse maneuver is related to the time-to-rendezvous in the manner shown in figure 19. The ratio of fuel consumed in the line-of-sight maneuver to fuel consumed in a two-impulse rendezvous is plotted versus time-to-rendezvous in fractions of an orbital period. For example, regardless of initial range, a line-of-sight rendezvous taking half an orbital period would consume 5.27 times the fuel required to make a two-impulse transfer in the same time and from the same starting position. The fuel economy for the line-of-sight technique improves as the rendezvous times decrease and becomes comparable to the two-impulse fuel economy for rendezvous times less than about 5 minutes.

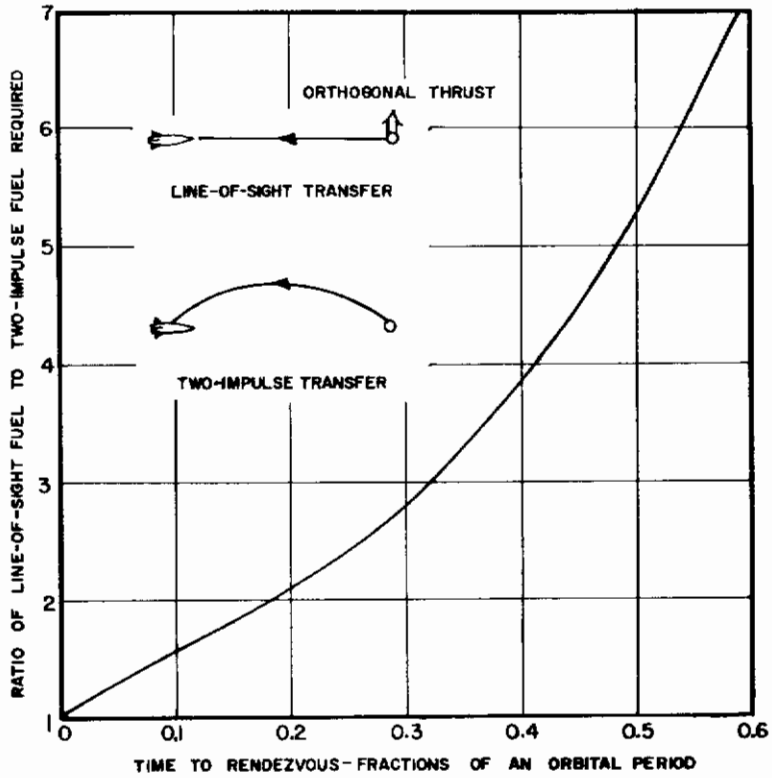

Figure 19. Comparison of Fuel Consumption for Line-of-Sight and Two-Impulse Rendezvous Techniques

It is interesting to note that Kasten's subjects (ref. 5) had so much difficulty trying to perform a two-impulse transfer using only visual cues that they ended up using more fuel than for a comparable line-of-sight rendezvous. This result indicates that the optimum technique would involve a combination of these two methods. The astronaut could estimate the correct aiming angle and coasting velocity (if properly trained) and embark on a two-impulse transfer. Due to aiming angle or velocity errors the trajectory would not be perfect. When it becomes apparent to the astronaut that he is not going to impact the target, he could begin a line-of-sight maneuver from that point, using orthogonal thrust to correct his path to a straight line and forward or retrothrust to control his closure velocity. Fuel required for such a technique should be more than that required for a two-impulse transfer but less than that required for a completely line-of-sight maneuver. Analog simulator studies to verify this concept are planned.

Rendezvous from Any Starting Position

To determine what effect initial position relative to the target has on the velocity and aiming angle required to make a two-impulse transfer, it is necessary to specify the initial position by means of an angle, α, where:

$$\tan \alpha = \frac{y_o}{x_o} \tag{34}$$

The aiming angle, θ, will still be defined as the angle between the line of sight to the target and the correct coasting velocity. If r_o is taken as the initial range to the target, then the correct x- and y-velocity components required to make a two-impulse transfer in a fraction of an orbital period given by p is:

$$\dot{x}_o = \omega r_o \cos\alpha \left\{ \frac{\tan\alpha[12\pi p - 14\tan(\pi p)] - 1}{8\tan(\pi p) - 6\pi p} \right\} \tag{35}$$

$$\dot{y}_o = \omega r_o \cos\alpha \left\{ \frac{\tan\alpha[6\pi p \cot(2\pi p) - 4] + 2\tan(\pi p)}{8\tan(\pi p) - 6\pi p} \right\} \tag{36}$$

Figure 20 shows how the aiming angle, θ, varies with initial position and time-to-rendezvous.

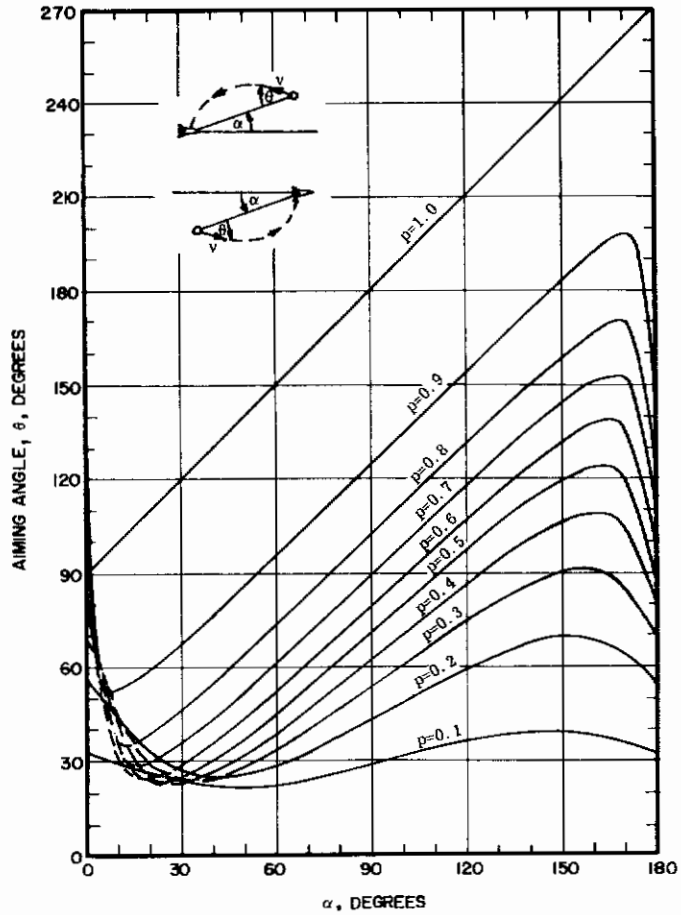

Figure 20. Aiming Angle as a Function of Starting Position and Rendezvous Time

The correct coasting velocity to intercept the target is plotted in figure 21. Examination of this chart reveals a rather surprising fact. For any starting position other than directly ahead of or behind the target (α = 0° or 180°), the velocity required for a two-impulse transfer approaches infinity as the time-to-rendezvous approaches one orbital period. Whereas it is possible to trade off velocity (and hence fuel) required against time when starting from a type I parking orbit, this trade-off is no longer possible if the interceptor starts from any other position. In other words, from directly ahead of or behind the target it is possible to make a two-impulse rendezvous with as low a velocity as desired. The price paid for this economy is a longer time-to-rendezvous. From any other position, however, there exists a minimum velocity below which rendezvous is impossible.

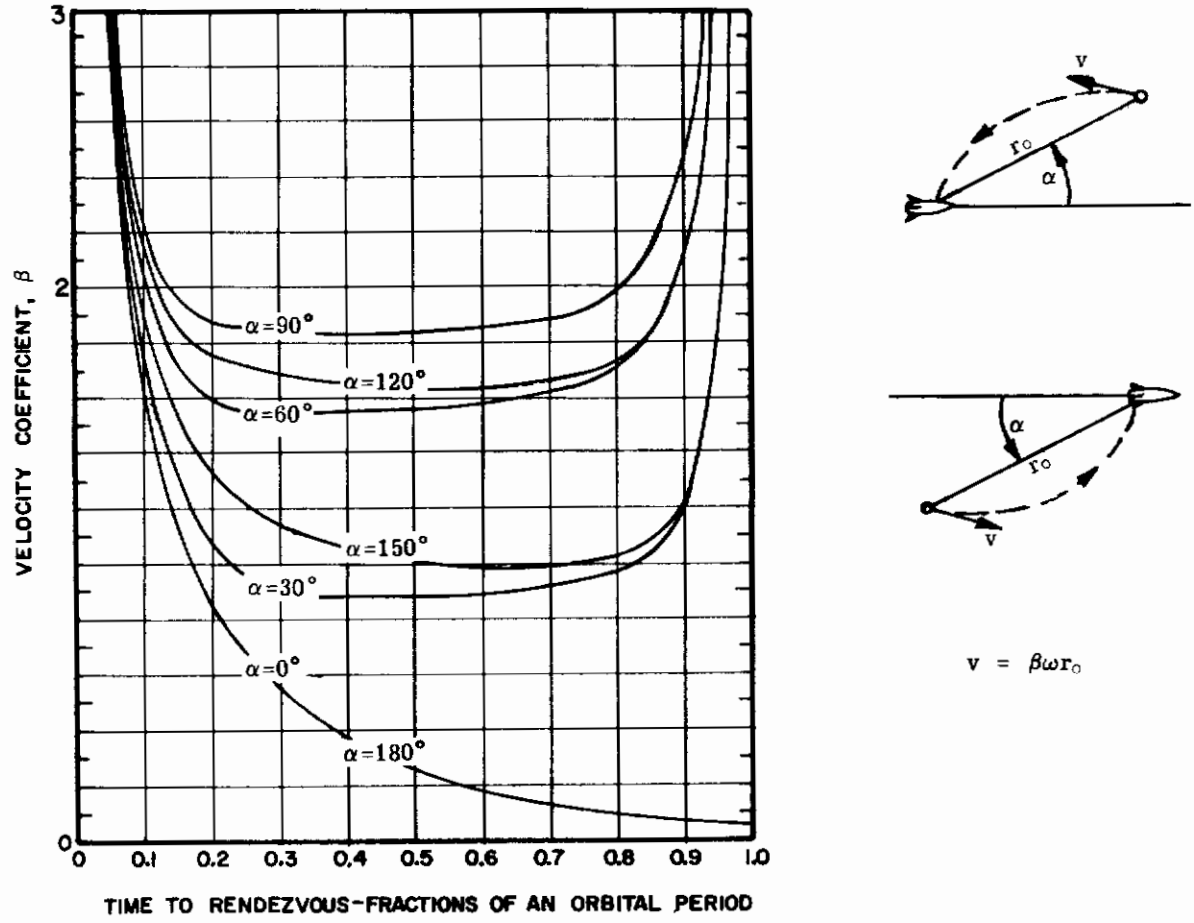

Figure 21. Initial Coasting Velocity as a Function of Starting Position and Rendezvous Time

The reason for this minimum velocity required for rendezvous lies in the fact that the tidal force field represents a potential barrier which the interceptor can overcome only at the expense of its velocity. In any rendezvous which involves a change in orbital altitude the interceptor must possess sufficient velocity to overcome this potential barrier. Hence, we note from figure 21 that starting positions directly above or below the target require the highest initial velocity.

The fuel required to make a two-impulse rendezvous is not directly proportional to the initial velocity. Since the total Δv consumed includes both the fuel required to accelerate the interceptor to its initial velocity and that required to decelerate it to rest at the target, any velocity lost as a result of changing orbital altitude represents a savings in deceleration fuel. It is well to keep in mind that in a rendezvous starting from any condition other than a type I parking orbit the interceptor will have a velocity relative to the target which is not zero. Therefore, it is impossible to specify the fuel required for a two-impulse transfer as a function of initial position without first specifying the exact parking orbit that the interceptor is in.

As an example of how the parking orbit affects the fuel required to rendezvous, consider type III orbits. Analysis reveals that two-impulse transfers starting from above and behind or from below and ahead of the target consume much more fuel than transfers starting from above and ahead or from below and behind the target. The reader will recognize that the latter conditions can be made to correspond to a Hohmann-type transfer.

The methods outlined in this report can be used to establish fuel requirements for any starting conditions. Knowing what the minimum two-impulse fuel required is for a particular starting condition and time-to-rendezvous gives the experimenter who is conducting rendezvous simulator studies a convenient yardstick against which he can measure the pilot's performance.

SECTION IV

CONCLUSIONS AND RECOMMENDATIONS

An interceptor vehicle's motion relative to a target in a circular or nearly circular orbit is influenced by a Coriolis acceleration which always acts in the orbital plane at right angles to the relative velocity vector, and by a tidal acceleration which always tends to push the interceptor away from the target's orbital altitude. The coasting trajectory of the interceptor which results from these accelerations can be described by a point moving around the perimeter of a 2 by 1 drifting ellipse.

The Coriolis acceleration cannot change the speed of the interceptor, but the tidal force field represents a potential energy barrier which changes the interceptor's speed as a function of orbital altitude.

Close-in parking orbits can be classified into four distinct categories according to whether the orbital period and eccentricity of the interceptor's orbit are the same or different from that of the target.

For the case where a pressure-suited man must exit the interceptor, travel to the target, and return, a type I parking orbit represents the most attractive starting condition. To enter a type I orbit the interceptor must position itself horizontally ahead of or behind the target and reduce its relative velocity to zero.

The recommended rendezvous technique for a man wearing a self-maneuvering unit and traveling from the interceptor in a type I orbit to the target is to estimate an aiming angle and initial coasting velocity which will result in a collision course with the target. After coasting to a point where the need for a correction becomes apparent, the man should initiate a line-of-sight transfer technique in which orthogonal thrust is used to keep him on the straight line course to the target.

In making a two-impulse transfer to the target from any position, the man must aim himself away from the target in a direction which depends only on the time he wishes to consume in coasting to the target regardless of the distance to be traveled. The correct initial coasting velocity also depends on the time-to-rendezvous and is directly proportional to the distance to be traveled.

Fuel requirements for short orbital transfers are determined primarily by the initial closure velocity with the target at the beginning of the rendezvous. However, all other factors being equal, a rendezvous from directly ahead of or behind the target consumes less fuel than a rendezvous started from above or below the target's orbital altitude.

Evaluating human and system performance during pilot-controlled rendezvous studies presents a problem because of the trade-offs which are possible between time and fuel consumption. The following procedure is proposed as a valid basis for rating human performance against a fixed standard: the time consumed in a pilot-controlled rendezvous should be measured and then the fuel required to perform a two-impulse transfer in the same time and with the same starting conditions should be determined by the methods outlined in this report. The ratio of the ideal fuel required to the actual fuel consumed is a direct measure of the efficiency of the pilot and control system in performing the rendezvous.

While the discussion in this report has centered around the problem of getting a pressure-suited man from an interceptor in a close-in parking orbit to a target, most of the findings are applicable to the more general problem of pilot-controlled rendezvous and docking. The technique of estimating an aiming angle for a two-impulse transfer would, however, not be applicable in the case in which a piloted interceptor is initially approaching the target from an arbitrary direction at some relatively high closure velocity. A different technique would be necessary to enable the astronaut to pilot the chase vehicle to a course which would intercept the target.

Undoubtedly, the terminal phase of rendezvous would be automatically controlled, at least until the pilot had visually acquired the target. The simplest terminal guidance schemes require thrust to nullify the angular velocity of the line of sight to the target, at the same time the closure velocity is reduced to zero at some arbitrarily small range. Fortunately, this would present the pilot with a convenient visual cue for checking the operation of the automatic guidance equipment since a nonrotating line of sight to the target would make the target appear stationary against the star background. Thus, the pilot could monitor the automatic system and take over manual control at any point after the target has been visually acquired—a task made more difficult by the lack of relative motion between target and background. The technique of nullifying the apparent drift of the target against the star background puts the interceptor very nearly on a coasting trajectory which intersects the target. The pilot would still be left with the range problem.

The problem of reducing high closure velocities prior to impact without reference to radar range and range-rate data is one which needs considerable work and should be the subject of future human engineering studies.

In addition, the nullifying of target drift against a star background presupposes the ability of the pilot to observe the stars in the presence of glare sources such as the sunlit earth and the target itself.

Optical devices intended to cope with the problems of dark adaptation in the presence of glare sources and visual ranging are under development in this laboratory and will be the subject of future reports.

LIST OF REFERENCES

1. Brissenden, R. F., B. Burton, E. Foudriat, and J. Whitten, Analog Simulation of a Pilot-Controlled Rendezvous, NASA TN D-747, National Aeronautics and Space Administration, Langley Research Center, Langley Field, Virginia, April 1961.

2. Gamow, G., "The Tides," Gravity, Chap 6, Anchor Books, Doubleday & Co., Inc., Garden City, Long Island, New York, 1962.

3. Griffin, J. B., Feasibility of a Self-Maneuvering Unit for Orbital Maintenance Workers, ASD Technical Documentary Report 62-278, Aeronautical Systems Division, Wright-Patterson Air Force Base, Ohio, February 1962.

4. Hord, R. A., Relative Motion in the Terminal Phase of Interception of a Satellite or a Ballistic Missile, NACA Technical Note 4399, National Advisory Committee for Aeronautics, Langley Aeronautical Laboratory, Langley Field, Virginia, September 1958.

5. Kasten, D. F., Human Performance for a Simulated Short Orbital Transfer, AMRL-TDR-62-138, 6570th Aerospace Medical Research Laboratories, Aerospace Medical Division, Wright-Patterson Air Force Base, Ohio, October 1962.

6. Meyer, W. A., A Method for Determining the Trajectories of Bodies Relative to a Satellite in a Circular Orbit, Report No. RE-1R-16, Chance Vought Research Center, Dallas, Texas, July 1961.

APPENDIX I

DERIVATION OF EQUATIONS OF MOTION

The coordinate frame defined in Section I is shown in figure 22 along with unit vectors $\hat{i}$, $\hat{j}$, and $\hat{k}$ extending along the x-, y-, and z- axes, respectively.

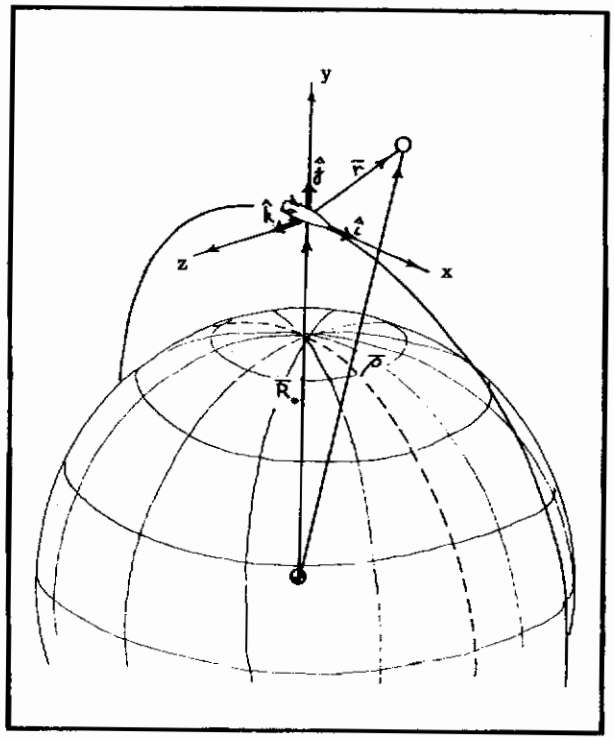

Figure 22. Definition of Vectors Used in Derivation of Equations of Motion

From figure 22 we see that:

$$\bar{\rho} = \bar{R}_o + \bar{r} \tag{37}$$

Since the target is acted upon by only the earth's gravitational attraction:

$$\ddot{\bar{R}}_o = -\mu \frac{\bar{R}_o}{R_o^3} = \frac{-\mu \hat{j}}{R_o^2} \tag{38}$$

where μ is the product of the universal gravitation constant and the mass of the earth.

Similarly:

$$\ddot{\bar{\rho}} = -\frac{\mu \bar{\rho}}{\rho^3} + \bar{f} \tag{39}$$

where $\bar{f}$ is the thrust force per unit mass acting on the interceptor.

If we assume that $r << \rho$, then:

$$\rho \simeq R_o + y \tag{40}$$

and since:

$$\bar{r} = x\hat{i} + y\hat{j} + z\hat{k} \tag{41}$$

then $\frac{\bar{\rho}}{\rho^3}$ in equation 39 becomes:

$$\frac{\bar{\rho}}{\rho^3} = \left[x\hat{i} + (R_o + y)\hat{j} + z\hat{k} \right] (R_o + y)^{-3} \tag{42}$$

Using the binomial expansion on the last factor of equation 42 and retaining only the first-order terms of the expansion reduces equation 42 to:

$$\frac{\bar{\rho}}{\rho^3} = \frac{x}{R_o^3}\hat{i} + \frac{(R_o + y)}{R_o^3}\hat{j} + \frac{z}{R_o^3}\hat{k} - \frac{3xy\hat{i}}{R_o^4} - \frac{3(R_o + y)y\hat{j}}{R_o^4} - \frac{3zy\hat{k}}{R_c^4}$$

Expanding and again discarding second-order terms yields:

$$\frac{\bar{\rho}}{\rho^3} = \frac{\bar{R}_o}{R_o^3} + \frac{1}{R_o^3}(x\hat{i} - 2y\hat{j} + z\hat{k}) \tag{43}$$

Substituting equation 43 into equation 39 we obtain:

$$\ddot{\bar{\rho}} = \ddot{\bar{R}}_o + \ddot{\bar{r}} = -\mu\left[\frac{\bar{R}_o}{R_o^3} + \frac{1}{R_o^3}(x\hat{i} - 2y\hat{j} + z\hat{k})\right] + \bar{f}$$

Substitution for $\ddot{\bar{R}}_o$ from equation 38 we obtain:

$$\ddot{\bar{r}} = \frac{-\mu}{R_o^3}(x\hat{i} - 2y\hat{j} + z\hat{k}) + \bar{f} \tag{44}$$

Equation 44 gives the inertial acceleration of the interceptor relative to the target. To obtain the acceleration relative to the rotating xyz-coordinate frame we must apply the Coriolis Theorem:

$$\left[\dot{\bar{r}}\right]_{\substack{\text{inertial}\\\text{frame}}} = \left[\dot{\bar{r}}\right]_{\substack{\text{rotating}\\\text{frame}}} + \bar{\omega} \times \bar{r} \tag{45}$$

where ω is the angular velocity of the xyz-coordinate frame.

If this is done, equation 44 reduces to the following three scalar equations:

$$\ddot{x} = \frac{-\mu}{R_o^3}x - 2\omega\dot{y} - \dot{\omega}y + \omega^2 x + f_x \tag{46}$$

$$\ddot{y} = \frac{2\mu}{R_o^3}y + 2\omega\dot{x} + \dot{\omega}x + \omega^2 y + f_y \tag{47}$$

$$\ddot{z} = \frac{-\mu}{R_o^3}z + f_z \tag{48}$$

If the target satellite is in a circular orbit, ω is a constant and:

$$\omega^2 = \frac{\mu}{R_o^3}$$

Equations 46, 47, and 48 reduce to:

$$\ddot{x} = -2\omega y + f_x \tag{1}$$

$$\ddot{y} = 2\omega\dot{x} + 3\omega^2 y + f_y \tag{2}$$

$$\ddot{z} = -\omega^2 z + f_z \tag{3}$$

which are the linearized equations of motion appearing in Section I.